

# Enhanced ferromagnetic and metal insulator transition in $\text{Sm}_{0.55}\text{Sr}_{0.45}\text{MnO}_3$ thin films: Role of oxygen vacancy induced quenched disorder

M. K. Srivastava,<sup>1,2</sup> P. K. Siwach,<sup>1</sup> A. Kaur,<sup>2</sup> and H. K. Singh<sup>1,a)</sup>

<sup>1</sup>National Physical Laboratory, CSIR, Dr. K. S. Krishnan Marg, New Delhi 110012, India

<sup>2</sup>Department of Physics and Astrophysics, University of Delhi, Delhi 110007, India

(Received 17 July 2010; accepted 1 October 2010; published online 3 November 2010)

Effect of quenched disorder (QD) caused by oxygen vacancy (OV) and substrate induced inhomogeneous compressive strain, on the magnetic and transport properties of oriented polycrystalline  $\text{Sm}_{0.55}\text{Sr}_{0.45}\text{MnO}_3$  thin films is investigated. QD is related intimately to the ordering/disordering of the OVs and controls the paramagnetic-ferromagnetic/insulator-metal transition. OV ordered films show enhanced  $T_C/T_{\text{IM}} \sim 165$  K, which is depressed by oxygen annealing. OV disordering realized by quenching reduces  $T_C/T_{\text{IM}}$ . The first order IM transition observed in SSMO single crystals is transformed into nonhysteretic and continuous one in the OV ordered films. QD appears to be diluted by OV disorder/annihilation and results in stronger carrier localization. © 2010 American Institute of Physics. [doi:10.1063/1.3505327]

$\text{Sm}_{1-x}\text{Sr}_x\text{MnO}_3$  ( $x=0.45$ ) occupies a unique position because it is very close to the charge order/orbital order (CO/OO) instability and shows the most abrupt insulator metal transition (IMT) among all manganites.<sup>1-3</sup> The ground states of the low bandwidth (W)  $\text{Sm}_{1-x}\text{Sr}_x\text{MnO}_3$  are (a) ferromagnetic metallic (FMM) at  $0.3 < x \leq 0.52$ , and (b) antiferromagnetic insulating (AFMI) for  $x > 0.52$ .<sup>1-3</sup> The CO occurs at  $0.4 \leq x \leq 0.6$  and the ordering temperature ( $T_{\text{CO}}$ ) increases from  $\sim 140$  to 205 K. Around  $x \approx 0.45$ , a very sharp (first order) transition from paramagnetic insulating (PMI) to the FMM state is observed in  $\text{Sm}_{0.55}\text{Sr}_{0.45}\text{MnO}_3$  (SSMO). At  $\sim 0.5$ ,  $\text{Sm}_{1-x}\text{Sr}_x\text{MnO}_3$  has a natural tendency toward phase separation (PS) that results in metamagnetism that provides intrinsic fragility to the composition-temperature ( $x$ - $T$ ) phase diagram vis-a-vis external perturbations.

Poly- and single-crystalline  $\text{Sm}_{1-x}\text{Sr}_x\text{MnO}_3$  have been studied in detail.<sup>2-6</sup> Unfortunately, thin films, either polycrystalline or epitaxial have not been studied in detail.<sup>7-9</sup> As reported earlier<sup>8,9</sup> the chief reason for this is the difficulty encountered in growth of good quality thin films. This is generally attributed to the extreme sensitivity of the electronic phases to the substrate induced pseudomorphic strains. It is generally accepted that the compressive strain favors FMM and the tensile strain enhances the AFM-COI fraction. In this letter we report the synthesis of highly oriented SSMO thin films on  $\text{LaAlO}_3$  (LAO)/(001) substrate. We also demonstrate that the magnetoelectrical properties are correlated strongly to the quenched disorder (QD) caused by coupled effect of substrate induced strain and oxygen vacancies (OVs).

Ultrasonic nebulized spray pyrolysis<sup>10</sup> was used to prepare polycrystalline SSMO thin films (thickness  $\sim 100$  nm) on single crystal LAO (001) substrates. Deposition conditions are the same as given by Agarwal *et al.*<sup>10</sup> One set of the films was annealed in air and the other in flowing oxygen, both at temperature  $T_A \sim 1273$  K for duration of 12 h followed by slow cooling. The third set was annealed in air and then rapidly cooled/quenched to room temperature

( $\sim 300$  K). The cooling rate for air and oxygen annealed films was  $4^\circ\text{C}/\text{min}$ . During quenching the samples were left under ambient condition to cool to room temperature. The structural and surface characterizations were performed by x-ray diffraction (XRD) and scanning electron microscopy, respectively. The cationic composition was studied by energy dispersive spectroscopy (EDS). The temperature and magnetic field dependent magnetization was measured by a commercial (Quantum Design) PPMS at 500 Oe magnetic field applied parallel to the film surface. The electrical resistivity was measured by the standard four probe technique.

The films annealed in air and oxygen will be designated as S-A and S-O, respectively while the quenched film will be denoted by S-Q. The XRD data (Fig. 1) shows that all the

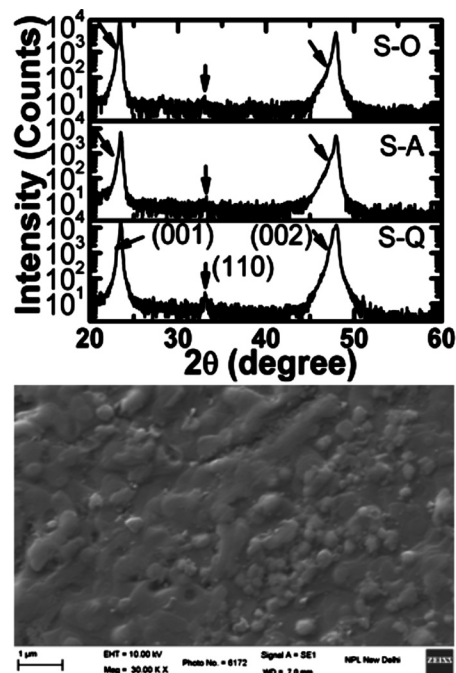


FIG. 1. XRD pattern of the S-O (top), S-A (middle), and S-Q (bottom) films. The SSMO reflections are indexed and marked. The lower panel shows the representative surface morphology of the film annealed in air.

<sup>a)</sup>Author to whom correspondence should be addressed. Electronic mail: hks65@nplindia.org.

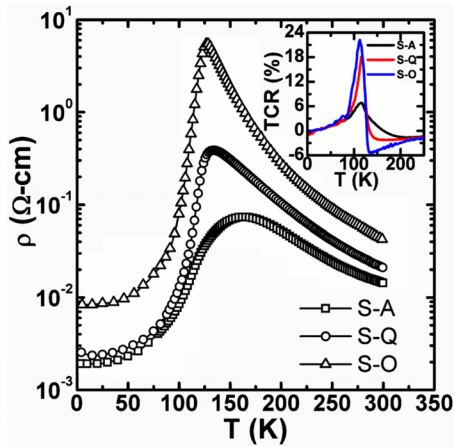


FIG. 2. (Color online) Temperature dependent resistivity of the SSMO films. The inset shows the temperature coefficient of resistivity of the three films.

films are single phase and strongly oriented along the out of plane direction. The out of plane (OP) lattice parameters ( $00\ell$ ) of the SSMO films almost coincide with that of the substrate LAO and remain nearly insensitive to the annealing conditions. The strong texturing suggests epitaxially grown regions, which could be separated by low angle grain boundaries (GBs). The structure of SSMO ( $x=0.45$ ) is orthorhombic (Pbnm) and the  $c$ -parameter corresponding to the cubic unit cell is  $c=3.83$  Å.<sup>2</sup> The S-A film has slightly larger OP lattice constant  $c_{S-A}=3.85$  Å, which decreases marginally in S-O and S-Q films. This suggests that all the films are under small compression, which is only weakly dependent on the annealing conditions. The closeness of the substrate and the film lattice parameters makes it difficult to unambiguously determine any effect of disorder freezing on the diffraction profile broadening. However, the pronounced appearance of the (110) reflection in the quenched samples may be suggestive of structural disorder. The surface of these films generally consists of large continuous layers having strong texturing and local epitaxial growth (see the lower panel of Fig. 1).

The temperature dependent resistivity ( $\rho-T$ ) of all the films is shown in Fig. 2. The IMT occurs at  $T_{IM}\approx 164$  K in the S-A films and is lowered to  $\sim 134$  K in S-Q films. The lowest  $T_{IM}\sim 128$  K is shown by the S-O films. The resistivity of S-A and S-O are, respectively, the lowest and the highest at all the temperatures and the latter has the sharpest IMT where the resistivity decreases by nearly three orders of magnitude between the  $T_{IM}$  and 4.2 K. In addition to the observed variation in resistivity and  $T_{IM}$ , the nature of the transition also shows a strong correlation with the annealing conditions. The nature of IMT is evaluated from the temperature coefficient of resistivity (TCR) [defined as  $TCR(\%)=d/dT(\ln \rho)\times 100$ ] depicted in the inset of Fig. 2. The peak TCR (peak temperature) value of S-A, S-Q, and S-O is found to be  $\approx 7\%$  (116 K),  $18\%$  (116 K), and  $22\%$  (112 K), respectively. Our S-A films show large enhancement in  $T_{IM}$  as compared to the polycrystalline/single crystalline bulk ( $T_{IM}\sim 130$  K) and thin films of similar composition.<sup>2-9</sup> However, the abrupt (first order) transition seen in single crystals<sup>1,2</sup> has been transformed into a continuous one in the S-A films. Hysteretic behavior of the  $\rho-T$  measured in heating-cooling cycles is also absent in the S-A films. But both S-O and S-Q films show hysteretic behavior (results not shown) that is

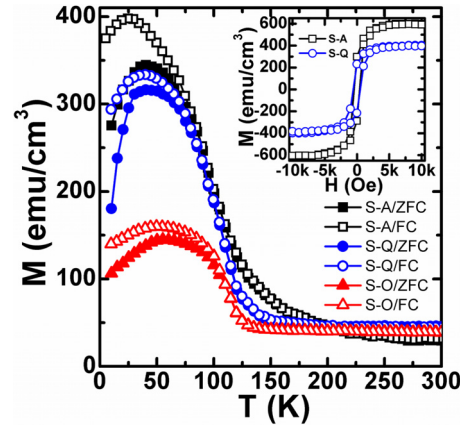


FIG. 3. (Color online) Temperature dependent ZFC (solid symbols)/FC (open symbols) magnetization of the SSMO films. The M-H loop of the S-A and S-Q film is inserted in the inset.

more pronounced in the latter. The difference in the  $T_{IM}$  measured during the two cycles is generally in the range 5–7 K. One possible reason for nonhysteretic and continuous IMT in S-A could be the presence of QD.<sup>11</sup>

The zero field cooled (ZFC) and field cooled (FC) magnetization data ( $M-T$ ) is shown in Fig. 3. Magnetization of the S-A film starts rising at  $T\approx 190$  K and then shows a FM transition at  $T_C\approx 165$  K, which like the IMT, is uncharacteristically broad for a low  $W$  compound like SSMO. Oxygen annealing and quenching, both lead to lower FM- $T_C\approx 130$  K and  $\approx 135$  K, respectively. At  $T<T_C$ , the ZFC and FC branches show strong divergence and at lower temperatures, the ZFC shows a sharp drop. This is a signature of a metamagnetic state, most likely a cluster glass (CG). The strongest ZFC-FC divergence and sharpest magnetization drop observed in the S-Q films show that they have the highest CG fraction. As seen in Fig. 3, the magnetic moment is lowered by quenching as well as oxygen annealing. The M-H loop of all the films shows small asymmetry in the coercivity ( $H_C$ ), which is found to be  $-435$  Oe and  $+408$  Oe for the S-A films, while the same for the S-Q films is  $-564$  Oe and  $+509$  Oe. The saturation moment ( $M_S$ ) is  $\approx 585$  emu/cm<sup>3</sup> and  $390$  emu/cm<sup>3</sup> for S-A and S-Q, respectively and the corresponding magnetic field ( $H_S$ ) is found to be  $\sim 4$  kOe. The asymmetric coercivity suggests the presence of exchange bias (EB) effect due to coexisting AFM and FM clusters. The M-H plots of the S-A and S-Q films are shown in the inset of Fig. 3. The quenching and oxygen annealing have following consequences on the SSMO films: (i) FM and IM transition temperature is lowered, (ii) FM and IM transition is sharpened, (iii) magnetic moment (also  $M_S$ ) is reduced, (iv)  $H_C$  increases, and (v) EB effect is enhanced.

The large enhancement in  $T_C/T_{IM}$  of the S-A films could be understood in terms of (i) the localized compressive strain and (ii) oxygen vacancy (OV) induced suppression of the AFM-COI state, which coexists with the PM/FMM. In SSMO, the coexistence of FMM and AFM-COI phases that leads to bicritical behavior is well established.<sup>1,2,11</sup> The COI clusters are present even in the PM phase ( $T>T_C$ ).<sup>11</sup> Due to the discontinuities at the GBs, the compressive strain is expected to be weak and spatially nonuniform. This is expected to act as inhomogeneity and could cause QD.<sup>11</sup> In manganites, the OVs can destabilize the COI phase both in single crystalline as well as polycrystalline materials quite

efficiently.<sup>10,12</sup> Since the oxygen stoichiometry is related to the effective hole concentration therefore even a mild inhomogeneity in the OV's could result in spatially varying carrier density that may also act as QD. In oriented polycrystalline thin films, the GB contribution is considerably reduced and the contribution of the QD is expected to be decisive. Thus OV's created due to high temperature air annealing coupled with the local compressive strain could act as the source of QD that in turn could transform the long range AFM-COI into short range and enhance the FMM fraction. This explains the observed rise in the magnetization at  $T > T_C$ . As  $T$  is lowered, the FMM fraction increases further and simultaneous PM-FM and IMT transitions occur ( $\sim 165$  K). The OV annihilation due to annealing can reduce the QD and hence lower  $T_C/T_{IM}$ . Here we must mention that the OV ordering plays important role in enhancing FMM properties. This is well accounted for by the characteristics shown by the S-Q films. Quenching freezes the randomly distributed OV's that transforms the correlated QD into uncorrelated one. Such a situation may be favorable for the growth of long range AFM-COI correlations at the cost of FMM ones. The carrier scattering is also enhanced due to disorder resulting in considerably higher resistivity and TCR as compared to the S-A films. Furthermore, the strong competition between these two phases in the vicinity of  $T_C/T_{IM}$  causes a bicritical like state. The FMM (AFM-COI) phase appears (disappears) abruptly at  $T_C$ . This explains the sharper IMT in the quenched films.

To unmask the substrate induced effects we prepared the SSMO films on (001) oriented SrTiO<sub>3</sub> (STO,  $a=3.905$  Å) and LSAT ( $a=3.868$  Å) substrates. The air annealed films on STO and LSAT have  $T_{IM}=105$  K and 130 K, respectively. The lowest  $T_{IM}=105$  K of the films on STO is due to the substrate induced tensile strain that favors the AFM-COI at the cost of FMM phase. Films on LSAT substrate are the least strained and have  $T_{IM}=130$  K. Quenching and oxygen annealing have the similar effect on these films as observed in the films on LAO. However, the films on STO show stronger decrease in  $T_C/T_{IM}$ . The lowering in  $T_C/T_{IM}$  of S-O films on all the substrates confirms that the enhancement is due to the OV's.

We also analyzed the electrical transport mechanism in the PM regime. The resistivity of the S-A and S-O films were best fitted by the Emin–Holstein<sup>13</sup> small polaron hopping (SPH) in the adiabatic limit, given by  $\rho(T) = AT \exp(E_A/k_B T)$  where the constant  $A$  is related to “ $n$ ” the polaron concentration; “ $a$ ” the site-to-site hopping distance, and “ $\nu$ ” the attempt frequency,  $k_B$  is the Boltzmann constant and  $E_A$  is the activation energy, which is approximated by  $E_A \approx E_p/2$ , the polaron binding energy.<sup>13</sup> The experimental  $\ln(\rho/T)$ - $1000/T$  plot and the fit to data is shown in Fig. 4. In case of S-A films, the deviation from the SPH is observed around  $T \sim 190$  K, which is well above the  $T_{IM}/T_C \approx 165$  K. In contrast, the SPH is valid down to  $T \sim 130$  K ( $T_{IM} \approx 128$  K) in the S-O film. As discussed earlier the appearance of FMM clusters in the PMI matrix ( $T > T_C$ ) causes the deviation from the SPH in S-A films. In case of S-O films the validity of SPH till the  $T_C/T_{IM}$  reconfirms that OV's are the major source of AFM-COI suppression and appearance of FMM clusters. Smaller value of  $E_A$  ( $\sim 91$  MeV) in S-A than S-O ( $\sim 114$  MeV) shows that the carriers are less local-

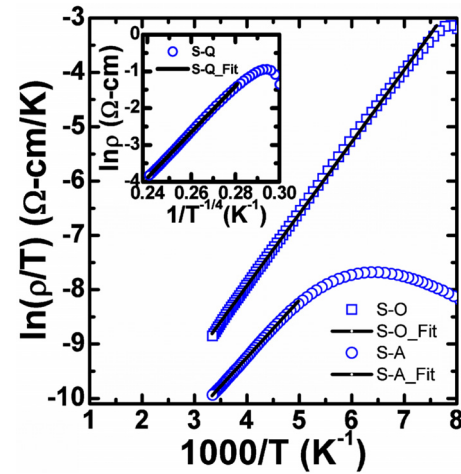


FIG. 4. (Color online) The main panel shows the experimental  $\ln(\rho/T)$ - $1000/T$  (SPH) plots (open symbols) and the fit (solid lines) to the data for S-A and S-O films. The inset shows the VRH plot of the experimental data and the corresponding fit (solid lines) for S-Q.

ized in the former. The resistivity of the S-Q could be fitted only with the Mott variable range hopping (VRH); given by  $\rho(T) = \rho_0 \exp(T_0/T)^{1/4}$ , where  $T_0$  is Mott's parameter (MP) giving a measure of the carrier localization.<sup>14</sup> The fitting range is  $T > 150$  K and the value of  $T_0 = 1.5 \times 10^7$  K. This value of MP corresponds to large activation energy ( $\sim 175$  meV) and is suggestive of very strong localization caused by the disorder and frozen OV's.

In summary, we have synthesized polycrystalline SSMO thin films and investigated the effect of the substrate induced strain and oxygen vacancy ordering/disordering on the magnetoelectric properties. The large enhancement in  $T_C/T_{IM}$  observed in films annealed in air has been explained as a consequence of correlated quenched disorder caused by the effect of spatially nonuniform strain and ordered oxygen vacancies. Quenched disorder is related to the ordering of oxygen vacancies and its impact is also reflected in the electrical transport in these films.

<sup>1</sup>Y. Tokura, *Rep. Prog. Phys.* **69**, 797 (2006).

<sup>2</sup>Y. Tomioka, H. Hiraka, Y. Endoh, and Y. Tokura, *Phys. Rev. B* **74**, 104420 (2006).

<sup>3</sup>C. Martin, A. Maignan, M. Hervieu, and B. Raveau, *Phys. Rev. B* **60**, 12191 (1999).

<sup>4</sup>A. Rebello and R. Mahendiran, *Appl. Phys. Lett.* **93**, 232501 (2008).

<sup>5</sup>M. Egilmez, K. H. Chow, J. Jung, and Z. Salman, *Appl. Phys. Lett.* **90**, 162508 (2007).

<sup>6</sup>M. Egilmez, K. H. Chow, J. Jung, I. Fan, A. I. Mansour, and Z. Salman, *Appl. Phys. Lett.* **92**, 132505 (2008).

<sup>7</sup>H. Oshima, K. Miyano, Y. Konishi, M. Kawasaki, and Y. Tokura, *Appl. Phys. Lett.* **75**, 1473 (1999).

<sup>8</sup>M. Kasai, H. Kuwahara, Y. Tomioka, and Y. Tokura, *J. Appl. Phys.* **80**, 6894 (1996).

<sup>9</sup>M. Egilmez, M. Abdelhadi, Z. Salman, K. H. Chow, and J. Jung, *Appl. Phys. Lett.* **95**, 112505 (2009).

<sup>10</sup>V. Agarwal, R. Prasad, M. P. Singh, P. K. Siwach, A. Srivastava, P. Fournier, and H. K. Singh, *Appl. Phys. Lett.* **96**, 052512 (2010).

<sup>11</sup>E. Dagotto, *New J. Phys.* **7**, 67 (2005).

<sup>12</sup>N. N. Loshkareva, N. V. Mushnikov, A. V. Korolyov, and E. A. Neifeld, *Phys. Rev. B* **77**, 052406 (2008).

<sup>13</sup>R. Prasad, M. P. Singh, P. K. Siwach, W. Prellier, A. Kaur, and H. K. Singh, *J. Appl. Phys.* **103**, 083906 (2008).

<sup>14</sup>P. K. Siwach, H. K. Singh, and O. N. Srivastava, *J. Phys.: Condens. Matter* **18**, 9783 (2006).